Protein kinase Cβ as a therapeutic target stabilizing blood–brain barrier disruption in experimental autoimmune encephalomyelitis

Tobias V. Lanz[a,b], Simon Becker[a], Matthias Osswald[b,c], Stefan Bittner[d], Michael K. Schuhmann[d], Christiane A. Opitz[a,b], Sadanand Gaikwad[a], Benedikt Wiestler[b,c], Ulrike M. Litzenburger[a,b], Felix Sahm[e,f], Martina Ott[a,b], Simeon Iwantscheff[a,b], Carl Grabitz[a,b], Michel Mittelbronn[g], Andreas von Deimling[e,f], Frank Winkler[b,c], Sven G. Meuth[d], Wolfgang Wick[b,c], and Michael Platten[a,b,1]

German Cancer Consortium (DKTK) Clinical Cooperation Units [a]Neuroimmunology and Brain Tumor Immunology, [c]Neurooncology, and [e]Neuropathology, German Cancer Research Center (DKFZ), 69120 Heidelberg, Germany; [b]Department of Neurooncology and [f]Institute of Neuropathology, University Hospital Heidelberg, National Center for Tumor Diseases, 69120 Heidelberg, Germany; [g]Institute of Neurology (Edinger Institute), Goethe University, 60528 Frankfurt, Germany; [d]Department of Neurology, University of Münster, 48149 Münster, Germany

Edited by Lawrence Steinman, Beckman Center for Molecular Medicine, Stanford, CA, and accepted by the Editorial Board July 24, 2013 (received for review February 7, 2013)

Disruption of the blood–brain barrier (BBB) is a hallmark of acute inflammatory lesions in multiple sclerosis (MS) and its animal model experimental autoimmune encephalomyelitis. This disruption may precede and facilitate the infiltration of encephalitogenic T cells. The signaling events that lead to this BBB disruption are incompletely understood but appear to involve dysregulation of tight-junction proteins such as claudins. Pharmacological interventions aiming at stabilizing the BBB in MS might have therapeutic potential. Here, we show that the orally available small molecule LY-317615, a synthetic bisindolylmaleimide and inhibitor of protein kinase Cβ, which is clinically under investigation for the treatment of cancer, suppresses the transmigration of activated T cells through an inflamed endothelial cell barrier, where it leads to the induction of the tight-junction molecules zona occludens-1, claudin 3, and claudin 5 and other pathways critically involved in transendothelial leukocyte migration. Treatment of mice with ongoing experimental autoimmune encephalomyelitis with LY-317615 ameliorates inflammation, demyelination, axonal damage, and clinical symptoms. Although LY-317615 dose-dependently suppresses T-cell proliferation and cytokine production independent of antigen specificity, its therapeutic effect is abrogated in a mouse model requiring pertussis toxin. This abrogation indicates that the anti-inflammatory and clinical efficacy is mainly mediated by stabilization of the BBB, thus suppressing the transmigration of encephalitogenic T cells. Collectively, our data suggest the involvement of endothelial protein kinase Cβ in stabilizing the BBB in autoimmune neuroinflammation and imply a therapeutic potential of BBB-targeting agents such as LY-317615 as therapeutic approaches for MS.

EAE | enzastaurin | CNS

The central nervous system (CNS) is generally protected from insults by pathogens, toxic macromolecules, and encephalitogenic immune cells by the blood–brain barrier (BBB). Maintaining the integrity of the BBB on a cellular level requires the coordinated interaction of pericytes and endothelial and glial cells (1). On a molecular level, tight junctions (TJ) proteins form a complex network between endothelial cells to ensure BBB integrity (2). Several TJ-associated proteins with key functions have been identified including zona occludens (ZO) proteins, claudins, and occludin. In CNS diseases, particular tumors, and inflammation, the BBB is disrupted as a primary or a secondary event during disease evolution. In autoimmune inflammatory diseases of the CNS such as multiple sclerosis (MS), which is characterized by perivascular infiltrates of autoreactive, encephalitogenic T cells and subsequent demyelination and neuronal loss, BBB disruption is a hallmark of acute inflammatory lesions (3). Although the question whether BBB disruption is a primary or secondary event in lesion evolution is still a matter of debate, there is increasing evidence from studies of human MS plaques (4) and animal models of MS, such as experimental autoimmune encephalomyelitis (EAE), that the BBB integrity is disturbed as an early event preceding the influx of pathogenic T cells (5, 6). BBB disruption in inflammatory conditions of the CNS may result in permission of CNS penetrance of both cells and macromolecules, signified by leakage of contrast agents and perivascular inflammatory infiltrates in acute CNS lesion in MS and EAE.

A coordinated cascade is necessary to allow CNS infiltration of encephalitogenic T cells (7). Interaction of activated T cells with endothelial cells via cell-adhesion molecules appears to be a prerequisite for T-cell infiltration of the CNS, and targeting of cell adhesion is clinically used for the therapy of multiple sclerosis (8). The regulation and relevance of TJ-associated proteins in autoimmune neuroinflammation are far less understood. Although claudin 3 expression is lost in acute EAE in areas of inflammatory infiltrates (9), its pathophysiological relevance remains unclear. Conversely, induced expression of claudin 1 in cerebral endothelial cells ameliorates EAE (10). The expression of claudin 5 is suppressed in autoimmune neuroinflammation, and deficiency or down-regulation of claudin 5 results in increased BBB permeability (11–13), indicating that claudin 5 may be important in stabilizing BBB in EAE. On a cellular level, BBB integrity mediated by TJ proteins is controlled by astrocytes and pericytes (14–16). The molecular pathways regulating TJ-associated proteins are poorly understood but appear to involve G proteins, serine-, threonine-, and tyrosine-kinases, proteases, cytokines, intracellular calcium levels, and PKC (17). Common to most of these pathways is the modulation of cytoskeletal elements as well as connections of TJ transmembrane molecules to the cytoskeleton (18). Inhibition of PKCβ attenuates vascular permeability in the CNS via TJ proteins (19) and leads to

Author contributions: T.V.L., M. Osswald, W.W., and M.P. designed research; T.V.L., S. Becker, M. Osswald, S. Bittner, M.K.S., C.A.O., S.G., U.M.L., F.S., M. Ott, S.I., C.G., and M.M. performed research; M.M., A.v.D., F.W., S.G.M., and M.P. contributed new reagents/analytic tools; T.V.L., M. Osswald, C.A.O., B.W., F.S., M.M., and M.P. analyzed data; and T.V.L. and M.P. wrote the paper.

Conflict of interest statement: This research project has been supported by Eli Lilly and Company, Indianapolis, IN. The researchers have been free in their work but have received compound LY-317615 and financial support.

This article is a PNAS Direct Submission. L.S. is a guest editor invited by the Editorial Board.

Database deposition: The microarray data reported in this paper have been deposited in the Gene Expression Omnibus (GEO) database, www.ncbi.nlm.nih.gov/geo (accession no. GSE48572).

[1]To whom correspondence should be addressed. E-mail: michael.platten@med.uni-heidelberg.de.

This article contains supporting information online at www.pnas.org/lookup/suppl/doi:10.1073/pnas.1302569110/-/DCSupplemental.

a lower permeability of tight junctions in an in vitro model of aglycemic hypoxia (20). In rat brains, PKCβ inhibition prevents the leakage of BBB induced by electromagnetic pulse (21). In addition, PKCβ is induced in endothelial cells under inflammatory conditions (22). To test the hypothesis that pharmacological interference with BBB stability might constitute a valuable therapeutic approach in autoimmune neuroinflammation, we analyzed the efficacy and mechanism of action of LY-317615, a small-molecule inhibitor of PKCβ, in EAE.

Results

Inhibition of PKCβ by LY-317615 Ameliorates EAE. To evaluate whether PKCβ is a potential therapeutic target in autoimmune neuroinflammation, we treated immunized SJL mice with the proteolipid protein peptide 139–151 ($PLP_{139–151}$) to develop relapsing–remitting EAE with the orally active PKCβ inhibitor LY-317615 using 50 $mg·kg^{-1}·day^{-1}$. This treatment resembles doses used in human studies, calculated according to FDA guidelines (23), and it is comparable with what has previously been used in animal models of cancer (24). To mimic a clinically relevant setting (25), once daily oral gavage of LY-317615 was initiated at the peak of disease at day 14 after immunization. Treatment with LY-317615 led to a substantial and sustained suppression of clinical disease relapse (Fig. 1*A*). Histopathologic analyses of the spinal cords revealed reduction of inflammatory infiltrates and increased preservation of myelin in the LY-317615–treated vs. the sham-treated group receiving vehicle only (Fig. 1*B*), indicating that LY-317615 suppresses clinical disease activity by suppressing CNS inflammation and demyelination. T-cell proliferation and cytokine production was unspecifically suppressed even in the absence of an antigenic stimulus in LY-317615–treated animals (Fig. S1). Subset analyses of $CD4^+$ lymph-node cells did not reveal differences between control and treatment groups (Fig. S1), and myelin-specific T-cell activation was not compromised. In fact, the proliferation index of PLP-activated lymph node cells was increased in the LY-317615 group (Fig. S1). Detailed analyses of in vitro T-cell proliferation confirmed unspecific effects on T-cell activation by various TCR stimuli associated with decreased phosphorylation of glycogen synthase kinase 3β (GSK3β), the molecular target of LY-317615 downstream of PKCβ, at relevant concentrations (Fig. S1). Of note, LY-317615 did not induce cell death in T cells (Fig. S2). Collectively, these data suggest that, whereas LY-317615 unspecifically suppressed T-cell proliferation, myelin-specific T cells appeared to be retained in the periphery.

LY-317615 Suppresses CNS Infiltration of Myelin-Specific T Cells. We then tested the hypothesis that myelin-specific T cells are not the therapeutic target of LY-317615 in EAE. Adoptive transfer of ex vivo activated PLP-specific T cells into LY-317615–treated recipient mice revealed a profound amelioration of clinical disease activity (Fig. 1*C*) and a strong suppression of inflammatory demyelination (Fig. 1*D*), supporting the hypothesis that LY-317615 compromises the ability of activated myelin-specific T cells to infiltrate the CNS. When LY-317615 treatment was used in a different EAE model that requires opening of the BBB using pertussis toxin, LY-317615 was ineffective with respect to both clinical disease activity (Fig. 1*E*) and inflammatory demyelination (Fig. S3) despite similar unspecific effects on T-cell proliferation. These data suggested that LY-317615 ameliorates neuroinflammation by suppressing the influx of encephalitogenic T cells into the CNS.

LY-317615 Targets Endothelial Cells to Suppress T-Cell Migration. We next tested the hypothesis that LY-317615 suppresses the transendothelial migration of T cells using an in vitro migration model. Although pretreatment of activated T cells did not alter the penetration of an endothelial cell monolayer, pretreatment of mouse-brain microvascular endothelial cells (MBMEC) was sufficient to compromise the transmigration of activated T cells (Fig. 2*A*), indicating that endothelial cells are the target of LY-317615–mediated suppression of T-cell transmigration. Treatment of MBMEC with LY-317615 did not alter secretion of the chemokines IFN induced protein 10 (IP-10) and monocyte chemotactic protein 1 (MCP-1/CCL-2) (Fig. 2*B*). In contrast, mRNA expression of the TJ-associated proteins ZO-1, claudin 3, and particularly claudin 5, but not intracellular adhesion molecule (ICAM), was induced (Fig. 2*C*). Induction of claudin 5 protein expression was confirmed using immunofluorescent staining of MBMEC (Fig. 2 *D* and *E*). This induction suggests that LY-317615–mediated suppression of transendothelial migration of activated T cells is—at least in part—mediated by up-regulation of TJ-associated proteins and stabilization of the BBB. To identify potential additional mechanisms involved in the inhibition of transendothelial leukocyte migration, gene-expression analyses of inflamed primary MBMEC treated with LY-317615 were performed in vitro. Indeed, these analyses revealed a more complex inhibition of leukocyte transendothelial migration pathways involving the suppression of additional key targets such as the Rho GTPase family member Rac1, which is induced by PKCβ (26) and has been shown to be critically involved in immunomodulatory efficacy of IFN-β in EAE (27), or the Rap guanine nucleotide exchange factor (GEF) 3 (Rapgef3), which is critically involved in the inflammatory vascular permeability (28). In addition, there was down-regulation of the transforming growth factor (TGF)-β pathway, which is induced during endothelial inflammation via PKCβ (29), and which is—when active in the CNS during autoimmune neuroinflammation—critical for the recruitment of encephalitogenic T cells (30, 31) (Fig. S4). Collectively, these data indicate that targeting PKCβ with LY-317615 modulates critical signaling pathways in inflamed endothelial cells to suppress transendothelial leukocyte migration.

LY-317615 Reduces BBB Breakdown in EAE. To investigate the effect of LY-317615 treatment on the BBB integrity in vivo, we analyzed the leakage of Evans Blue into CNS tissue after systemic injection in mice with EAE. Although in naïve animals Evans Blue was retained in the systemic circulation, in animals with EAE CNS, inflammation led to a profound leakage of Evans Blue in spinal cord tissue. This leakage was reduced in animals treated with LY-317615 (Fig. 3*A*). In addition, two-photon microscopy of cerebellar brain vessels after systemic injection of fluorescently labeled dextran confirmed that LY-317615 treatment suppressed BBB breakdown associated with autoimmune neuroinflammation in vivo (Fig. 3 *B* and *C*). These data suggested that LY-317615 stabilizes the BBB, which is disrupted in the acute phase of EAE. This BBB-stabilizing effects of LY-317615 indeed resulted in the inhibition of transendothelial T-cell migration in vivo as demonstrated by immunohistochemical visualization of T cells in spinal-cord sections of animals with EAE. These analyses revealed that $CD3^+$ T cells were largely restricted to blood vessels ("confined") in LY-317615–treated animals whereas, in control-treated animals, inflammatory lesions were more dispersed ("spread") (Fig. 3 *D* and *E*).

LY-317615 Up-Regulates TJ-Associated Proteins in Vivo. We next analyzed the mechanism involved in preventing BBB breakdown by LY-317615 treatment. LY-317615 led to an up-regulation of vessel-associated claudin 5 expression in the spinal cord (Fig. 4 *A* and *B*). Notably, ultrastructural analyses revealed no profound differences in TJ morphology in LY-317615–treated animals (Fig. 4*C*), which is in line with previous reports demonstrating that inhibition of PKCβ does not compromise the structural integrity of TJ (22). Collectively, these data suggest that LY-317615 prevents autoimmune neuroinflammation by stabilizing the disrupted BBB via up-regulation of claudin 5, thus limiting the influx of encephalitogenic T cells.

Discussion

Here, we show that the clinically used PKCβ inhibitor LY-317615 is effective in ameliorating disease activity in EAE, an experimental model of MS (Fig. 1*A*). It reduces inflammation and

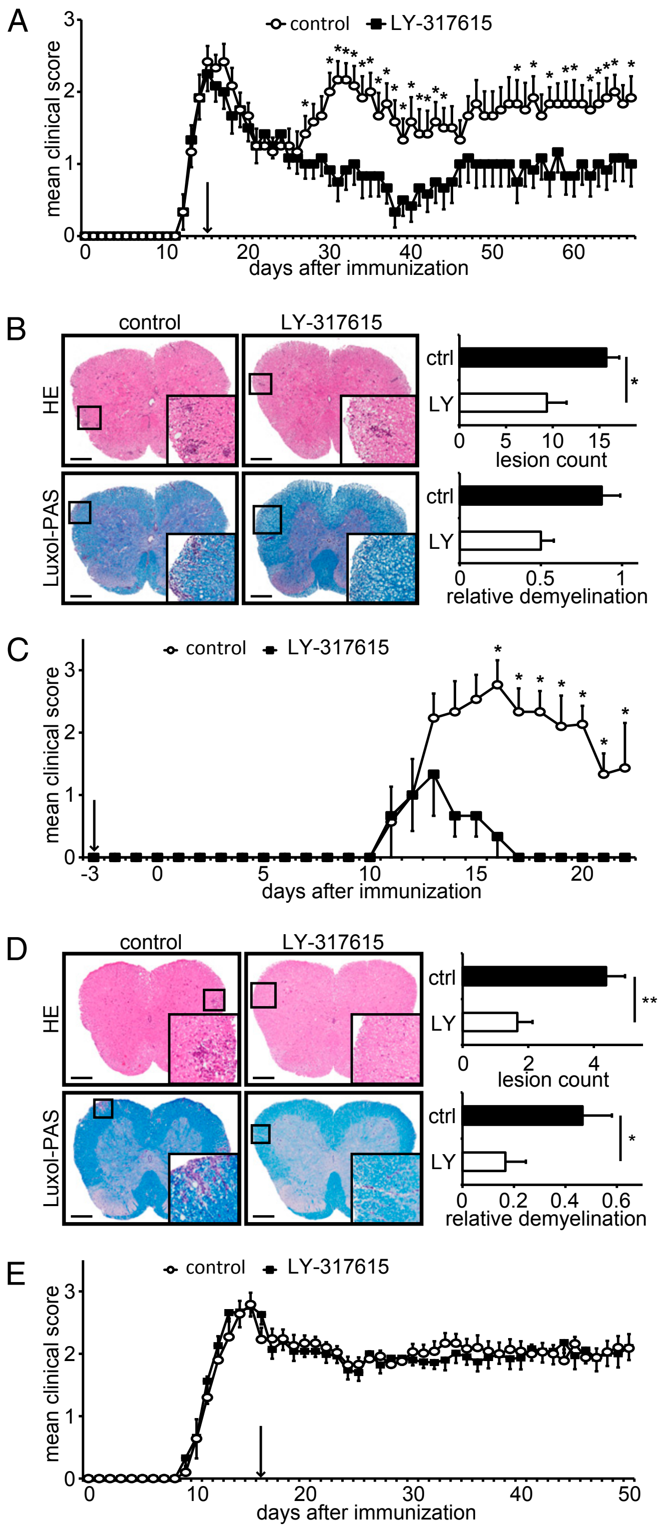

Fig. 1. LY-317615 treatment is effective in $PLP_{139–151}$-induced EAE. (*A*) Daily disease scores of SJL mice immunized with $PLP_{139–151}$. Daily oral application of LY-317615 was initiated at the peak of disease (arrow). One representative experiment is shown out of four independent experiments with 10 mice per group, respectively. $*P < 0.05$ according to Mann–Whitney *U* test. (*B*) H&E-stained (*Upper*) and Luxol-PAS–stained (*Lower*) slides of spinal cords from diseased SJL mice and their statistical evaluation. Representative slides are shown, and statistics were obtained from at least five mice per group. $*P < 0.05$ according to Student *t* test. (Scale bars: 200 μm.) (*C*) Daily disease scores of EAE in SJL mice, induced by adoptively transferred LN cells from immunized mice after 72 h of restimulation in vitro. Recipient mice were treated daily with LY-317615, starting 3 d before cell transfer (arrow). One representative experiment is shown out of three independent experiments with five mice per group, respectively. $*P < 0.05$ according to Mann–Whitney *U* test. (*D*) H&E-stained (*Upper*) and Luxol-PAS–stained (*Lower*) slides of spinal cords from diseased animals and their statistical evaluation. Representative slides are shown, and statistics were obtained from at least five mice per group. $*P < 0.05$ according to Student *t* test. (Scale bars: 200 μm.) (*E*) Daily disease scores of EAE in C57BL/6 mice, immunized with $MOG_{35–55}$ and injected twice with 200 ng per mouse pertussis toxin. LY-317615 treatment started at the peak of disease (arrow). One representative experiment is shown out of two independent experiments with 10 mice per group, respectively. $*P < 0.05$ according to Mann–Whitney *U* test.

demyelination (Fig. 1*B*) by targeting endothelial and possibly astrocytic PKCβ, resulting in a stabilization of the BBB. Therefore, this orally active compound may constitute an interesting and novel approach to prevent and treat inflammatory activity in MS, which is different from the currently available immunomodulatory agents.

Therapeutic approaches to MS classically target the T-cell compartment based on genetic and histopathological evidence and functional studies in MS and EAE, suggesting that MS is an autoimmune disease mainly driven by encephalitogenic $CD4^+$ T cells (32). The therapeutic efficacy of drugs solely suppressing the activation and/or proliferation of $CD4^+$ T cells, however, has been limited. Broadly immunosuppressive approved agents such as mitoxantrone are only second-line agents also because their long-term safety profile does not justify implementation as first-line agents compared with more tolerable baseline therapies such as β-interferons or glatiramer acetate. However, also more specific anti–T-cell agents, such as depleting αCD4 antibodies, have largely failed in clinical trials, with the exception of alemtuzumab, a monoclonal αCD52 antibody (33). More advanced therapeutic approaches to MS target the transmigration of encephalitogenic T cells without disturbing the T-cell activation. These agents typically target T cells directly, such as natalizumab acting on VLA4 on T cells to suppress transendothelial transmigration (34).

We provide here evidence for the potential of targeting endothelial cells rather than T cells to suppress transendothelial migration of encephalitogenic T cells. Our data provide evidence that LY-317615 ameliorates EAE by directly stabilizing the BBB, as pretreatment of endothelial cells but not activated T cells in an in vitro model leads to suppression of lymphocyte transmigration (Fig. 2*A*) and treatment of mice with LY-317615 results in stabilization of the BBB during neuroinflammation by macroscopic (Evans Blue) and microscopic (two-photon microscopy) criteria (Fig. 3 *A*–*C*). Importantly, the stabilization of BBB was associated with an increase in vessel-associated $CD3^+$ T cells in mice with EAE in contrast to more dispersed T-cell infiltrates in control-treated mice, suggesting that LY-317615 treatment results in a retention of CNS-infiltrating T cells (Fig. 3 *D* and *E*). Direct proof, however, that the stabilization of the BBB is the only mechanism of action in EAE is not possible based on our data. LY-317615 results in a suppression of T-cell proliferation and cytokine production in vitro, not only after antigen-specific stimulation but also after TCR stimulation (Fig. S2), indicating that LY-317615 also targets T-cell activation directly. Interestingly, however, the frequency of myelin-specific T cells in mice immunized with PLP in the periphery after treatment with LY-317615 is increased (Fig. S1). This observation also indicates that encephalitogenic T cells are retained in the periphery due to the BBB-stabilizing effects of LY-317615. This hypothesis is further supported by the observation that LY-317615 does not affect disease activity when the BBB is artificially disrupted by pertussis toxin (Fig. 1*E*). Although pertussis toxin is very effective in permeabilizing an intact BBB (35) and thus allowing myelin-specific T cells to enter the CNS, other mechanisms by which pertussis toxin promotes neuroinflammation

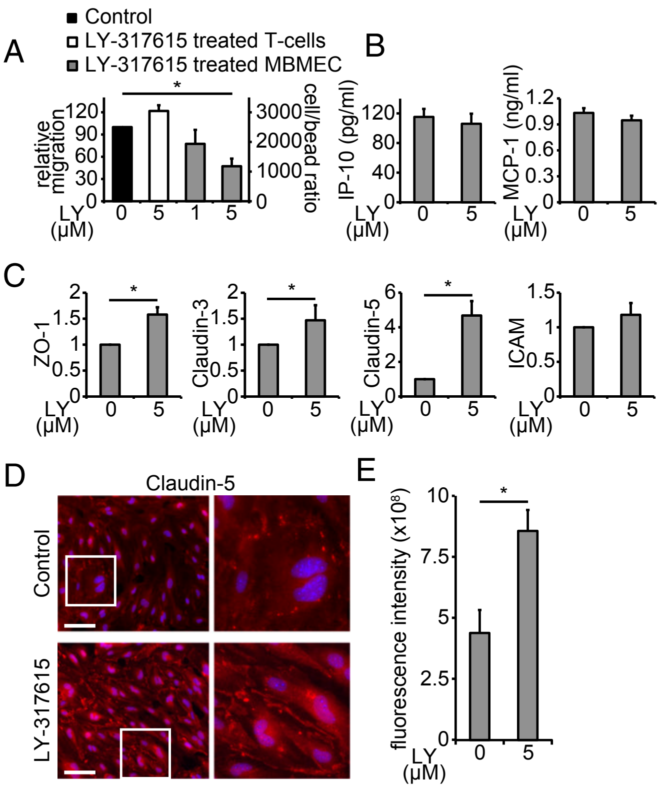

Fig. 2. LY-317615 stabilizes tight junctions in brain endothelial cells. (*A*) Migration of T cells through a monolayer of MBMECs was measured by flow cytometry. Untreated control migration (black) was compared with migration when T cells (white) or MBMECs (gray) were separately treated with LY-317615. Data represent mean ± SEM from four independent experiments. **P* < 0.05 according to Student *t* test. (*B*) MBMEC-derived chemokines IP-10 and MCP-1 were detected using a fluorescent bead immunoassay. Data represent mean ± SEM from seven independent experiments. (*C*) qRT-PCR analysis of mRNA from MBMECs. Expression levels are shown in relation to the housekeeping gene GAPDH. (*A*–*C*) Data represent mean ± SEM from at least four independent experiments. **P* < 0.05 according to Student *t* test. (*D*) Immunofluorescence images for claudin 5 of cultured MBMEC, stimulated for 24 h with 5 μM LY-317615. Images shown are representative pictures out of six per group from three biological replicates. (*E*) Statistical evaluation of the claudin 5 immunofluorescence images shown in *D*; mean fluorescence intensity was measured after background substraction. Data represent mean ± SEM from six slides per group of three biological replicates. **P* < 0.05 according to Student *t* test.

in EAE have been suggested (36). Therefore, the fact that LY-317615 is ineffective when pertussis toxin is used may well be attributed to other anti-inflammatory properties blunted by pertussis toxin. There is, however, evidence that PKCβ, the molecular target of LY-317615, is implicated in BBB stabilization. In fact, the permeabilization of the BBB by pertussis toxin involves PKC (37).

Although the disruption of the BBB has been recognized as a hallmark of acute and chronic MS plaques for decades, it has not been in the focus of drug development, mainly because the molecular mechanisms that are responsible for BBB disruption in MS had been incompletely understood. Although mediators from infiltrating T cells such as the T helper cytokine interleukin-17 (IL-17) are certainly capable of sustaining BBB disruption in inflammatory lesions (38), the question whether BBB disruption precedes infiltration of pathogenic T cells and which factors are responsible for this disruption remains controversial. Increasing evidence suggests that the TJ-associated protein claudin 5 expressed in endothelial cells is a key determinant in BBB stability in EAE and MS. Claudin 5 is highly expressed in brain endothelial cells (9) and necessary to ensure BBB integrity (39, 40). Expression of claudin 5 is decreased in the acute phase of EAE (12). In line with the notion that the loss of claudin 5 expression critically contributes to the BBB breakdown in EAE, our data demonstrate that the therapeutic efficacy of LY-317615 is associated with an increased claudin 5 expression (Fig. 4 *A* and *B*). Although we have not observed ultrastructural BBB changes evoked by LY-317615 (Fig. 4*C*), its molecular target, PKCβII, leads to a lower permeability of tight junctions (20) and contributes to BBB disruption (21).

Given the favorable safety profile of this drug in oncology trials (41), even in brain tumors (42), our results suggest potential efficacy of LY-317615 in MS patients. Based on its propensity to inhibit tumor-cell proliferation, induce apoptosis in tumor cells, and block tumor-induced angiogenesis (43), LY-317615 has been

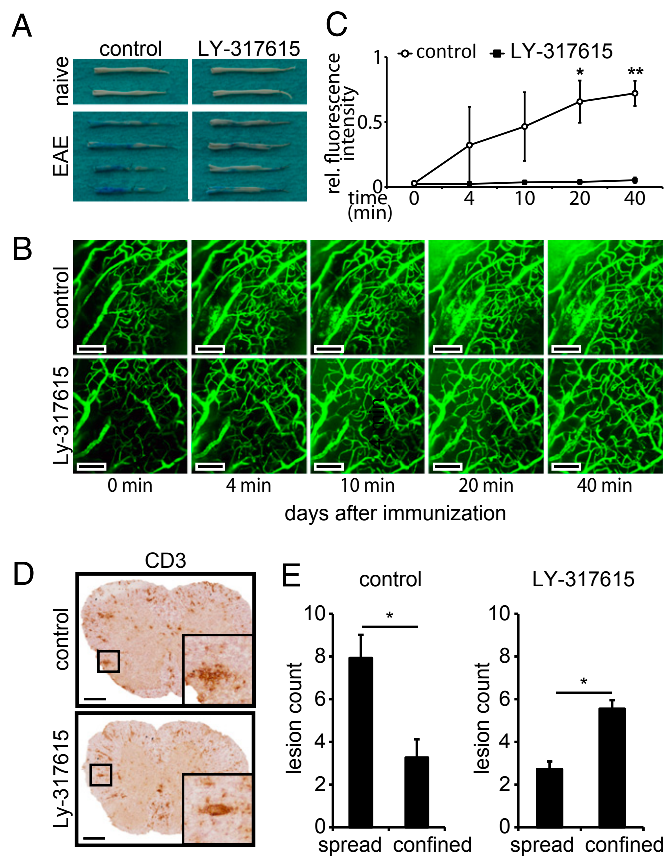

Fig. 3. LY-317615 seals the blood–brain barrier in vivo. (*A*) Macroscopic pictures of spinal cords (front and back side) of one naïve mouse (*Upper*) and two diseased mice (*Lower*) per group, killed at the peak of disease. Evans Blue had been injected 1 h before euthanization. Spinal cords shown are representative pictures from two independent experiments with five mice per group, respectively. (*B*) Two-photon microscopy of diseased mice. Pictures were taken at the indicated time points after dextran infusion. Picture series are representative for two mice per group; each mouse was investigated at several parts of the brain. (Scale bars: 100 μm.) (*C*) Statistical evaluation of two-photon images. Fluorescence intensity was measured in leaky spots near blood vessels and compared with fluorescence intensity inside the corresponding vessel. Mean ± SEM are shown from three independent spots per group. **P* < 0.05 and ***P* < 0.005 according to Student *t* test. (*D*) Immunohistochemistry for CD3 of inflamed spinal cords from diseased SJL mice treated with control (*Upper*) or LY-317615 (*Lower*). Representative images are shown from five mice per group. (Scale bars: 200 μm.) (*E*) Statistical analysis of the slides shown in *D*; lesions >10 cells were counted and divided into spread lesion and confined lesion groups according to blinded morphological analysis. Mean ± SEM are shown from at least three slides of five mice per group. **P* < 0.05 according to Student *t* test.

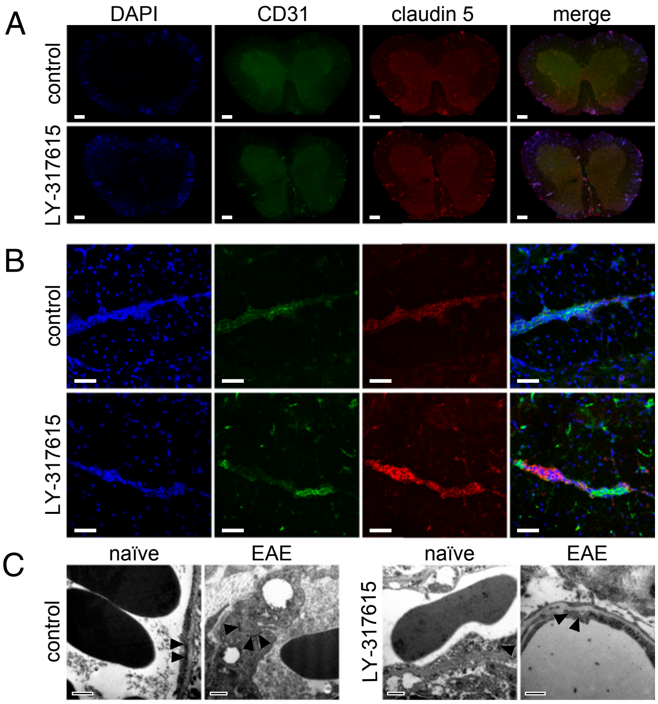

Fig. 4. Expression of claudin 5 in EAE tissue. (*A*) Fluorescent immunohistological staining for CD31 (green) and claudin 5 (red) in spinal cords from diseased SJL mice treated with control (*Upper*) or LY-317615 (*Lower*). Slides from one representative animal are shown out of five individuals. (Scale bars: 200 μm.) (*B*) Confocal images of single inflamed vessels in spinal cords from diseased SJL mice treated with control (*Upper*) or LY-317615 (*Lower*), stained for CD31 (green) and claudin 5 (red). Images are representative from one out of five animals. (Scale bars: 50 μm.) (*C*) Electromicroscopical pictures of spinal cords from naïve (naïve) and diseased (EAE) SJL mice treated with control vehicle (*Left*) or LY-317615 (*Right*). Tight junctions are pointed out by triangular arrows. (Scale bars: 500 nm.)

tested in first- and second-line clinical trials in several cancers, including lymphoma and glioblastoma, with a dose of 525 mg/day (44) with promising results mainly in B-cell lymphomas (45, 46). Although PKCβ has been demonstrated to facilitate intestinal sugar absorption (47) and synaptic transmission (48) and learning-related signal transduction (49), treatment of patients with glioblastoma with LY-317615 resulted in manageable side effects that included nausea, dizziness, fatigue, convulsion, diarrhea, thrombocytopenia, liver-enzyme elevations, hypernatremia, and deep-vein thrombosis (42). PKCβ is blocked by LY-317615 with high specificity by competing with ATP for the enzyme's ATP-binding site with a 50% inhibitory concentration (IC_{50}) of 6 nmol/L. Other PKCs are inhibited off target, but at higher IC_{50} (50). The best-studied pathways affected by PKCβ are the activation of the MAPK/Erk pathway via phosphorylation of Ras (26) and the phosphorylation of AKT at Ser^{473}, which is essential for AKT activity (51). Both AKT and PKCβ phosphorylate GSK3β. Detection of nonphosphorylated GSK3β is the most reliable marker for the pharmacological activity of LY-317615 (50). Indeed, kinase assays in mouse and human endothelial cells confirm GSK3β as the prime target of LY-317615, with only the protooncogene tyrosine-protein kinase Fyn—to a lesser extent—suppressed in both species (Fig. S5), indicating limited off-target effects in endothelial cells. Using GSK3β phosphorylation, we also demonstrate biological activity of LY-317615 at therapeutic concentrations in T cells (Fig. S1*G*).

Collectively, our data demonstrate that the high-affinity PKCβ inhibitor LY-317615 reduces inflammation and demyelination in an animal model of MS most likely by suppressing endothelial and astrocytic PKCβ, resulting in stabilizing the BBB via claudin 5 and subsequent suppression of T-cell infiltration. Targeting the BBB by an orally available drug may be a promising strategy for the treatment of diseases associated with an inflammatory BBB disruption such as MS.

Materials and Methods

Animals. Female 8- to 12-wk-old SJL mice (Janvier) as well as C57BL/6J mice (Charles River) were used throughout the study. All animal work was performed in accordance with the German animal protection law under the permission of the local authorities in Heidelberg and Karlsruhe.

EAE. SJL mice were immunized s.c. with 100 μg per mouse proteolipid protein peptide 139–151 ($PLP_{139–151}$), and C57BL/6 mice were immunized with the same amount of myelin oligodendrocyte glycoprotein peptide 35–55 ($MOG_{35–55}$) (both from the Peptide Synthesis Core Facility of the DKFZ), emulsified in complete Freund's Adjuvant (Difco) containing 200 μg of *Mycobacterium tuberculosis* (Difco). C57BL/6 mice received 200 ng per mouse pertussis toxin (List Biological Laboratories Inc.) i.p. on the day of immunization and 2 d thereafter. Clinical signs of disease were scored daily according to a standard scoring system (0, no clinical signs; 1, loss of tail tone; 2, hind limb weakness; 3, complete hind limb paralysis; 4, hind limb and forelimb paralysis; and 5, moribund or dead). Mice were treated daily by oral gavage with 1.25 mg per mouse LY-317615 (kindly provided by Lilly), dissolved in 0.5% methyl cellulose. Control animals received the equal volume of methyl cellulose.

T-Cell Proliferation and Cytokine Measurement. Naïve mice were used for antigen-unspecific proliferation. For antigen-specific proliferation of T cells, mice were killed on day 9 after immunization with $PLP_{139–151}$. Cells were isolated as described earlier (31). Briefly, lymph node cells were mechanically singularized and seeded in U-bottom 96-well plates (TPP) at 5×10^5 cells per well in enriched RPMI. Naïve lymph node cells were stimulated with either Phytohemagglutinin (PHA) (Sigma-Aldrich) at 1 μg/mL, phorbol 12-myristate 13-acetate (PMA) and ionomycin (both from Sigma) at 20 ng/mL / 1 μg/mL, or antibodies to CD3 and CD28 (BD Biosciences) at 1 μg/mL / 10 μg/mL, and Con A (Sigma) at 2 μg/mL. Lymph node cells from previously immunized animals were reactivated with 5–20 μg/mL $PLP_{139–151}$. For measurement of T-cell proliferation, cells were pulsed after 72 h with ^{3}H-methylthymidine (Amersham-Pharmacia Biotech) at 1 μCi per well for the last 18 h. Cells were harvested using a Tritium Harvester (Tomtec) and a β-plate reader (Wallac) with BetaWin software. For cytokine measurements, supernatants were taken up after 72 h of culture and measured by ELISA for the cytokines IL-2, IL-4, IL-6, IL-10, IL-17A, and IFN-γ (ebioscience), according to the manufacturer's instructions.

Transendothelial Migration Assays. Transmigration of $CD4^+$ cells through an in vitro BBB model was assessed as described before (52, 53). In brief, MBMEC were prepared from brains of C57BL/6 mice and cultured 5 d before use on 3.0-μm ColagenIV/fibronectin-coated Transwell Pore Polyester Membrane inserts (Corning). Purity, confluence, and cell morphology were checked regularly by microscopy. T cells from C57BL/6 mice were loaded in the upper chamber of a Transwell with or without a MBMEC monolayer. After an incubation period of 18 h, migrated cells from the lower chamber were collected and counted (membrane without MBMEC monolayer) or Calibrite beads (BD Biosciences) were added. The number of migrated cells was determined by flow cytometry and is presented as cell per bead ratio as internal calibration standard. For calibration purposes, T-cell migration was measured without MBMEC layer showing no effect of LY-317615 (Fig. S6).

Fluorescent Immunocytochemistry. MBMEC were seeded 1 wk after preparation on glass coverslips. After treatment with 5 μM LY-317615 for 24 h, cells were fixed with 4% (vol/vol) PFA for 10 min at room temperature and then permeabilized with Acetone for 10 min at −20 °C and stained with rabbit anti-claudin 5 antibody (Invitrogen) according to standard protocols. Microscopy images were taken using an NiE inverted automated microscope (Nikon). Statistical analysis was done using Fiji software (54). After subtraction of background staining intensity, mean fluorescent intensity was measured.

ACKNOWLEDGMENTS. This work was supported by Helmholtz Foundation Grant VH-NG-306 (to M.P.), German Research Foundation Grant SFB938 TPK (to M.P. and W.W.), and the German Research Foundation (§91b) (W.W. and F.W.). Eli Lilly provided LY-317615 and funds for kinase profiling and microarray analyses. T.V.L. and C.O. were funded by the postdoctoral program of the Heidelberg University Medical Faculty, S.I. was funded by the doctorate program of the German Research Foundation (SFB938), and C.G. was funded

MEDICAL SCIENCES

by the doctorate program of the Hartmut Hoffmann-Berling International Graduate School of Molecular and Cellular Biology of the Universities of Heidelberg/Mannheim. S.G.M. was funded by the Interdisciplinary Center for Clinical Research (IZKF) Münster (Meu3/010/12).

1. Takeshita Y, Ransohoff RM (2012) Inflammatory cell trafficking across the blood-brain barrier: Chemokine regulation and in vitro models. *Immunol Rev* 248(1):228–239.
2. Coisne C, Engelhardt B (2011) Tight junctions in brain barriers during central nervous system inflammation. *Antioxid Redox Signal* 15(5):1285–1303.
3. Alvarez JI, Cayrol R, Prat A (2011) Disruption of central nervous system barriers in multiple sclerosis. *Biochim Biophys Acta* 1812(2):252–264.
4. Gaitán MI, et al. (2011) Evolution of the blood-brain barrier in newly forming multiple sclerosis lesions. *Ann Neurol* 70(1):22–29.
5. Bennett J, et al. (2010) Blood-brain barrier disruption and enhanced vascular permeability in the multiple sclerosis model EAE. *J Neuroimmunol* 229(1-2):180–191.
6. Fairless R, et al. (2012) Preclinical retinal neurodegeneration in a model of multiple sclerosis. *J Neurosci* 32(16):5585–5597.
7. Lyck R, Engelhardt B (2012) Going against the tide—how encephalitogenic T cells breach the blood-brain barrier. *J Vasc Res* 49(6):497–509.
8. Engelhardt B, Ransohoff RM (2005) The ins and outs of T-lymphocyte trafficking to the CNS: Anatomical sites and molecular mechanisms. *Trends Immunol* 26(9):485–495.
9. Wolburg H, et al. (2003) Localization of claudin-3 in tight junctions of the blood-brain barrier is selectively lost during experimental autoimmune encephalomyelitis and human glioblastoma multiforme. *Acta Neuropathol* 105(6):586–592.
10. Pfeiffer F, et al. (2011) Claudin-1 induced sealing of blood-brain barrier tight junctions ameliorates chronic experimental autoimmune encephalomyelitis. *Acta Neuropathol* 122(5):601–614.
11. Errede M, et al. (2012) Blood-brain barrier alterations in the cerebral cortex in experimental autoimmune encephalomyelitis. *J Neuropathol Exp Neurol* 71(10):840–854.
12. Wang C, et al. (2013) Immune-related GTPase Irgm1 exacerbates experimental autoimmune encephalomyelitis by promoting the disruption of blood-brain barrier and blood-cerebrospinal fluid barrier. *Mol Immunol* 53(1-2):43–51.
13. Argaw AT, Gurfein BT, Zhang Y, Zameer A, John GR (2009) VEGF-mediated disruption of endothelial CLN-5 promotes blood-brain barrier breakdown. *Proc Natl Acad Sci USA* 106(6):1977–1982.
14. Liebner S, et al. (2008) Wnt/beta-catenin signaling controls development of the blood-brain barrier. *J Cell Biol* 183(3):409–417.
15. Daneman R, et al. (2009) Wnt/beta-catenin signaling is required for CNS, but not non-CNS, angiogenesis. *Proc Natl Acad Sci USA* 106(2):641–646.
16. Alvarez JI, et al. (2011) The Hedgehog pathway promotes blood-brain barrier integrity and CNS immune quiescence. *Science* 334(6063):1727–1731.
17. Muldoon LL, et al. (2013) Immunologic privilege in the central nervous system and the blood-brain barrier. *J Cereb Blood Flow Metab* 33(1):13–21.
18. Wolburg H, Lippoldt A (2002) Tight junctions of the blood-brain barrier: Development, composition and regulation. *Vascul Pharmacol* 38(6):323–337.
19. Willis CL, Meske DS, Davis TP (2010) Protein kinase C activation modulates reversible increase in cortical blood-brain barrier permeability and tight junction protein expression during hypoxia and posthypoxic reoxygenation. *J Cereb Blood Flow Metab* 30(11):1847–1859.
20. Kim YA, et al. (2010) Role of PKCbetaII and PKCdelta in blood-brain barrier permeability during aglycemic hypoxia. *Neurosci Lett* 468(3):254–258.
21. Qiu LB, et al. (2010) The role of protein kinase C in the opening of blood-brain barrier induced by electromagnetic pulse. *Toxicology* 273(1-3):29–34.
22. Rigor RR, Hawkins BT, Miller DS (2010) Activation of PKC isoform beta(I) at the blood-brain barrier rapidly decreases P-glycoprotein activity and enhances drug delivery to the brain. *J Cereb Blood Flow Metab* 30(7):1373–1383.
23. FDA (2005) *Guidance for Industry: Estimating the Maximum Safe Starting Dose in Initial Clinical Trials for Therapeutics in Adult Healthy Volunteers* (Center for Drug Evaluation and Research, Rockville, MD).
24. Tabatabai G, et al. (2007) Synergistic antiglioma activity of radiotherapy and enzastaurin. *Ann Neurol* 61(2):153–161.
25. Platten M, et al. (2005) Treatment of autoimmune neuroinflammation with a synthetic tryptophan metabolite. *Science* 310(5749):850–855.
26. Zhang J, Anastasiadis PZ, Liu Y, Thompson EA, Fields AP (2004) Protein kinase C (PKC) betaII induces cell invasion through a Ras/Mek-, PKC iota/Rac 1-dependent signaling pathway. *J Biol Chem* 279(21):22118–22123.
27. Inoue M, et al. (2012) Interferon-β therapy against EAE is effective only when development of the disease depends on the NLRP3 inflammasome. *Sci Signal* 5(225):ra38.
28. Parnell E, et al. (2012) Regulation of the inflammatory response of vascular endothelial cells by EPAC1. *Br J Pharmacol* 166(2):434–446.
29. Xu Y, et al. (2010) Blockade of PKC-beta protects HUVEC from advanced glycation end products induced inflammation. *Int Immunopharmacol* 10(12):1552–1559.
30. Luo J, et al. (2007) Glia-dependent TGF-beta signaling, acting independently of the TH17 pathway, is critical for initiation of murine autoimmune encephalomyelitis. *J Clin Invest* 117(11):3306–3315.
31. Lanz TV, et al. (2010) Angiotensin II sustains brain inflammation in mice via TGF-beta. *J Clin Invest* 120(8):2782–2794.
32. Zamvil SS, Steinman L (2003) Diverse targets for intervention during inflammatory and neurodegenerative phases of multiple sclerosis. *Neuron* 38(5):685–688.
33. Coles AJ, et al. (2012) Alemtuzumab more effective than interferon β-1a at 5-year follow-up of CAMMS223 clinical trial. *Neurology* 78(14):1069–1078.
34. Steinman L (2009) A molecular trio in relapse and remission in multiple sclerosis. *Nat Rev Immunol* 9(6):440–447.
35. Linthicum DS (1982) Development of acute autoimmune encephalomyelitis in mice: Factors regulating the effector phase of the disease. *Immunobiology* 162(3):211–220.
36. Weber MS, et al. (2010) Repetitive pertussis toxin promotes development of regulatory T cells and prevents central nervous system autoimmune disease. *PLoS ONE* 5(12): e16009.
37. Brückener KE, el Bayâ A, Galla HJ, Schmidt MA (2003) Permeabilization in a cerebral endothelial barrier model by pertussis toxin involves the PKC effector pathway and is abolished by elevated levels of cAMP. *J Cell Sci* 116(Pt 9):1837–1846.
38. Huppert J, et al. (2010) Cellular mechanisms of IL-17-induced blood-brain barrier disruption. *FASEB J* 24(4):1023–1034.
39. Saitou M, et al. (2000) Complex phenotype of mice lacking occludin, a component of tight junction strands. *Mol Biol Cell* 11(12):4131–4142.
40. Liebner S, Kniesel U, Kalbacher H, Wolburg H (2000) Correlation of tight junction morphology with the expression of tight junction proteins in blood-brain barrier endothelial cells. *Eur J Cell Biol* 79(10):707–717.
41. Wick W, et al. (2011) Pathway inhibition: Emerging molecular targets for treating glioblastoma. *Neuro-oncol* 13(6):566–579.
42. Wick W, et al. (2010) Phase III study of enzastaurin compared with lomustine in the treatment of recurrent intracranial glioblastoma. *J Clin Oncol* 28(7):1168–1174.
43. Ma S, Rosen ST (2007) Enzastaurin. *Curr Opin Oncol* 19(6):590–595.
44. Carducci MA, et al. (2006) Phase I dose escalation and pharmacokinetic study of enzastaurin, an oral protein kinase C beta inhibitor, in patients with advanced cancer. *J Clin Oncol* 24(25):4092–4099.
45. Morschhauser F, et al. (2008) A phase II study of enzastaurin, a protein kinase C beta inhibitor, in patients with relapsed or refractory mantle cell lymphoma. *Ann Oncol* 19(2):247–253.
46. Robertson MJ, et al. (2007) Phase II study of enzastaurin, a protein kinase C beta inhibitor, in patients with relapsed or refractory diffuse large B-cell lymphoma. *J Clin Oncol* 25(13):1741–1746.
47. Kellett GL (2001) The facilitated component of intestinal glucose absorption. *J Physiol* 531(Pt 3):585–595.
48. Fioravante D, Chu Y, Myoga MH, Leitges M, Regehr WG (2011) Calcium-dependent isoforms of protein kinase C mediate posttetanic potentiation at the calyx of Held. *Neuron* 70(5):1005–1019.
49. Weeber EJ, et al. (2000) A role for the beta isoform of protein kinase C in fear conditioning. *J Neurosci* 20(16):5906–5914.
50. Graff JR, et al. (2005) The protein kinase Cbeta-selective inhibitor, Enzastaurin (LY317615.HCl), suppresses signaling through the AKT pathway, induces apoptosis, and suppresses growth of human colon cancer and glioblastoma xenografts. *Cancer Res* 65(16):7462–7469.
51. Kawakami Y, et al. (2004) Protein kinase C betaII regulates Akt phosphorylation on Ser-473 in a cell type- and stimulus-specific fashion. *J Biol Chem* 279(46):47720–47725.
52. Göbel K, et al. (2011) Blockade of the kinin receptor B1 protects from autoimmune CNS disease by reducing leukocyte trafficking. *J Autoimmun* 36(2):106–114.
53. Weidenfeller C, Schrot S, Zozulya A, Galla HJ (2005) Murine brain capillary endothelial cells exhibit improved barrier properties under the influence of hydrocortisone. *Brain Res* 1053(1-2):162–174.
54. Schindelin J, et al. (2012) Fiji: An open-source platform for biological-image analysis. *Nat Methods* 9(7):676–682.